

# Tunable Optomechanically Induced Sideband Comb

Jun-Hao Liu,<sup>1</sup> Ya-Fei Yu,<sup>2</sup> Guangqiang He,<sup>3</sup> Qin Wu,<sup>4</sup> Jin-Dong Wang,<sup>2,\*</sup> and Zhi-Ming Zhang<sup>1,†</sup>

<sup>1</sup>*Guangdong Provincial Key Laboratory of Nanophotonic Functional Materials and Devices  
(School of Information and Optoelectronic Science and Engineering),  
South China Normal University, Guangzhou 510006, China*

<sup>2</sup>*Guangdong Provincial Key Laboratory of Quantum Engineering and Quantum Materials,  
South China Normal University, Guangzhou 510006, China*

<sup>3</sup>*State Key Laboratory of Advanced Optical Communication Systems and Networks,  
Department of Electronic Engineering, Shanghai Jiao Tong University, Shanghai 200240, China*

<sup>4</sup>*School of Biomedical Engineering, Guangdong Medical University, Dongguan 523808, China*

Cavity optomechanical system (COMS) can exhibit optical frequency comb (OFC) effect when it is driven by a control field  $\omega_c$  and a probe field  $\omega_p$ , and works in the non-perturbative regime. For such a comb, its repetition frequency is equal to the mechanical frequency  $\omega_b$  and is untunable. Here we address this problem by driving the system with an additional strong probe field  $\omega_f$ , and the detuning between  $\omega_f$  and  $\omega_c$  is equal to  $\omega_b/n$ , i.e., a fraction of the mechanical frequency. In this case, we obtain some interesting results. We find that not only the integer-order (higher-order) sidebands, but also the fraction-order sidebands, as well as the sum and difference sidebands between the integer- and fraction-order sidebands, will appear in the output spectrum. The generated nonlinear sidebands constitute an optomechanically induced sideband comb (OMISC). The frequency range and the repetition frequency of OMISC are proportional to the sideband cutoff-order number and the sideband interval, respectively. We show that we can extend the sideband cutoff-order number and sequentially enlarge the frequency range of OMISC by increasing the intensity of the probe field  $\omega_p$ . More importantly, we can decrease the sideband interval, and in turn, the repetition frequency of OMISC by increasing  $n$  and the intensity of the probe field  $\omega_f$ . Our work paves the way to achieve the tunable OFC based on COMS.

*Introduction-* Optical frequency comb (OFC) is known as the most accurate “ruler” on the earth [1]. Ever since proposed by Chebotayev [2] and Hänsch [3] in 1970s, it has attracted a lot of attention in many study and application areas, such as tests of fundamental physics with atomic clocks [4], calibration of atomic spectrographs [5], precision time and frequency transfer [6], coherent optical communication [7], molecular fingerprinting [8], precision ranging [9], and so on. The original OFC source is a phase-stabilized mode-locked laser [10]. In the time domain the output field of such a mode-locked laser is present as a periodic train of ultrashort pulses, while in the frequency domain this pulse train can be transformed as a Fourier series of equidistant optical frequencies.

To support more and more broad application space, OFCs have experienced rapid changes over the past 20 years. A lot of new physical systems, such as fiber-based systems [11–13], semiconductor laser platforms [14, 15], microresonator systems [16–19], have been studied for achieving the tunable, miniaturized, and low-powered OFCs. More recently, efforts have also been made in cavity optomechanical system (COMS) [20–22]. An interesting effect named higher-order sideband generation (HSG) is discussed by Xiong et al., and they demonstrate that a higher-order sideband comb can be generated in an ultrastrong driven COMS beyond the perturbative approximation [23, 24].

If we consider an OFC as a “ruler”, the frequency range of the comb will be the length of the “ruler”, and the repetition frequency will be the minimum scale. For an

optomechanically induced sideband comb (OMISC), its frequency range is proportional to the sideband cutoff-order number and its repetition frequency is equal to the sideband interval. In previous works, people mainly focus on increasing the sideband cutoff-order number, for example, ones find that many physical effects and systems, such as Coulomb effect [25], atomic ensemble [26], Casimir effect [27], and parity-time symmetry structure [28], can effectively increase the cutoff-order number of the higher-order sideband output from COMS.

Unlike previous works, we are more interested in tuning or reducing the sideband interval. Actually in the output spectrum of COMS, the sideband interval is equal to the eigenfrequency of mechanical resonator, and we can decrease the sideband interval by reducing the mechanical frequency. However, owing to the limitation of the processing technology of optomechanical microcavity, it is hard to obtain a microcavity with a small mechanical frequency and a large optomechanical coupling strength. Therefore, ones must explore other ways to decrease the sideband interval.

In this letter, we address this problem by adding another probe field  $\omega_f$  into the proposal of Xiong et al. [23]. In particular, we assume that the detuning between  $\omega_f$  and  $\omega_c$  is equal to a fraction of the mechanical frequency  $\omega_b$ , i.e.,  $\omega_f - \omega_c = \omega_b/n$ . We find that not only the integer-order (higher-order) sidebands, but also the fraction-order sidebands, and the sum and difference sidebands between integer- and fraction-order sidebands, will appear in the output spectrum. The sideband in-

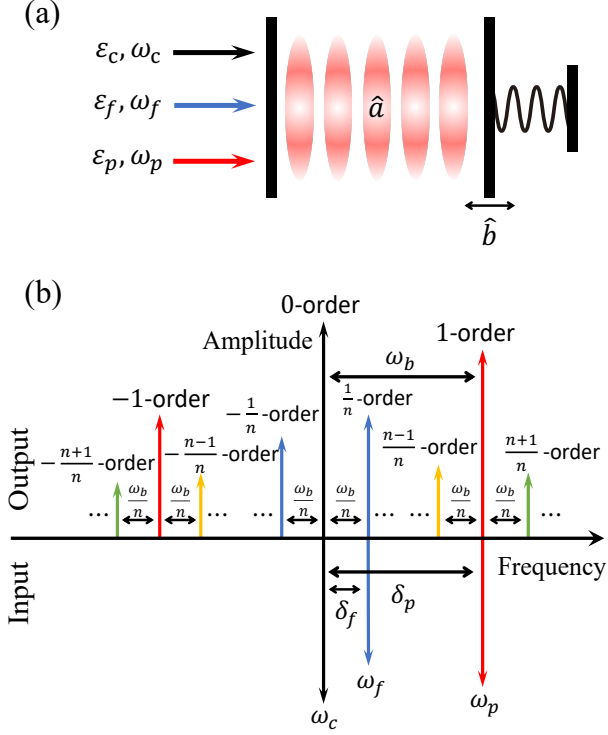


FIG. 1. (color online) (a) Standard cavity optomechanical system driven by a control field ( $\omega_c$ ) and two probe fields ( $\omega_p$ ,  $\omega_f$ ). (b) Schematic diagram of the nonlinear sideband generation. We exhibit the integer-order sidebands (0-order,  $\pm 1$ -order), the fraction-order sidebands ( $\pm \frac{1}{n}$ -order), the sum and difference sidebands ( $\pm \frac{n \pm 1}{n}$ -order).

interval is equal to  $\omega_b/n$ . So by increasing  $n$ , we can decrease the sideband interval, and in turn, the repetition frequency of OMISC.

*System model and Hamiltonian*- Our proposed scheme is shown in Fig. 1(a), we consider a standard model of COMS where an optical cavity mode  $\hat{a}$  parametrically couples with a mechanical mode  $\hat{b}$  via radiation pressure. The cavity mode is pumped by a control field  $\omega_c$  and two probe fields  $\omega_p$  and  $\omega_f$ . The Hamiltonian of the system is given by ( $\hbar = 1$ )

$$H = \omega_a \hat{a}^\dagger \hat{a} + \omega_b \hat{b}^\dagger \hat{b} + g \hat{a}^\dagger \hat{a} (\hat{b}^\dagger + \hat{b}) + i[\hat{a}^\dagger (\varepsilon_c e^{-i\omega_c t} + \varepsilon_p e^{-i\omega_p t} + \varepsilon_f e^{-i\omega_f t}) - H.c.], \quad (1)$$

where  $\hat{a}$  ( $\hat{a}^\dagger$ ) and  $\hat{b}$  ( $\hat{b}^\dagger$ ) are the bosonic annihilation (creation) operators for the cavity mode and the mechanical mode with frequencies  $\omega_a$  and  $\omega_b$ , respectively.  $g = x_{zpf} \omega_a / L$  is the single-photon optomechanical coupling strength where  $x_{zpf} = \sqrt{\hbar / 2M\omega_b}$  is the zero-point fluctuation,  $M$  is the mass of the mechanical oscillator and  $L$  is the length of the cavity. The amplitudes of the driving fields being  $\varepsilon_y = \sqrt{2\kappa P_y / \hbar \omega_y}$  ( $y = c, p, f$ ), in which  $\kappa$  denotes the cavity damping rate and  $P_y$  refers to the corresponding input power.

Based on the Hamiltonian (1), the evolution of the system can be described by the Heisenberg-Langevin equations (in a frame rotating at the frequency  $\omega_c$ ):

$$\dot{\hat{a}} = -(i\Delta_a + \kappa)\hat{a} - ig\hat{a}(\hat{b}^\dagger + \hat{b}) + \varepsilon_c + \varepsilon_p e^{-i\delta_p t} + \varepsilon_f e^{-i\delta_f t} + \sqrt{2\kappa}\hat{a}_{in}, \quad (2)$$

$$\dot{\hat{b}} = -(i\omega_b + \gamma)\hat{b} - ig\hat{a}^\dagger \hat{a} + \sqrt{2\gamma}\hat{b}_{in}, \quad (3)$$

where  $\Delta_a = \omega_a - \omega_c$  is the frequency detuning between the control field  $\omega_c$  and the cavity field  $\omega_a$ .  $\delta_p = \omega_p - \omega_c$  ( $\delta_f = \omega_f - \omega_c$ ) is the frequency detuning between the control field  $\omega_c$  and the probe field  $\omega_p$  ( $\omega_f$ ).  $\gamma$  is the mechanical damping rate.  $\hat{a}_{in}$  and  $\hat{b}_{in}$  are respectively the fluctuation operations corresponding to the cavity mode and the mechanical mode with zero mean value, i.e.,  $\langle \hat{a}_{in} \rangle = \langle \hat{b}_{in} \rangle = 0$ . We focus on the mean response of the system to the probe fields, thus in the following we turn to calculate the evolutions of the expectation values of the system operators  $\hat{a}$  and  $\hat{b}$ , and we denote  $\langle \hat{a} \rangle \equiv \alpha$ ,  $\langle \hat{b} \rangle \equiv \beta$ . By using the mean-field approximation, i.e.,  $\langle \hat{a}\hat{b} \rangle = \langle \hat{a} \rangle \langle \hat{b} \rangle$ , the dynamical equations of the system can be derived from Eqs.(2)-(3) as

$$\dot{\alpha} = -(i\Delta_a + \kappa)\alpha - ig\alpha(\beta + \beta^*) + \varepsilon_c + \varepsilon_p e^{-i\delta_p t} + \varepsilon_f e^{-i\delta_f t}, \quad (4)$$

$$\dot{\beta} = -(i\omega_b + \gamma)\beta - ig|\alpha|^2. \quad (5)$$

We recall that the solutions of the above nonlinear equations have been addressed in previous works for the following three parametric conditions: (i)  $\varepsilon_f = 0, \varepsilon_p \neq 0, \varepsilon_p / \varepsilon_c \ll 1$ , under this circumstance the equations can be solved by using the so-called linearization method, and the Stokes and anti-Stokes processes are discussed [29]. (ii)  $\varepsilon_f \neq 0, \varepsilon_p \neq 0, \varepsilon_p / \varepsilon_c \ll 1, \varepsilon_f / \varepsilon_c \ll 1$ , in this case the linearization is practicable, and the sum and difference sidebands effects are investigated [30, 31]. (iii)  $\varepsilon_f = 0, \varepsilon_p \neq 0, \varepsilon_p \sim \varepsilon_c$ , in this regime the linearization is inapplicable, and the higher-order sideband effect is studied by using the numerical calculation [23].

In this letter, we study the fourth circumstance, i.e.,  $\varepsilon_p \neq 0, \varepsilon_f \neq 0, \varepsilon_f \sim \varepsilon_p \sim \varepsilon_c$ , in this regime the expectation value  $x$  ( $x = \alpha, \beta$ ) can be written as

$$x = x_0 + x_p + x_f + x_s + x_d, \quad (6)$$

where  $x_0$  denotes the steady-state solution when  $\varepsilon_p = \varepsilon_f = 0$ . The optomechanical nonlinearity [corresponding to the terms  $-ig|\alpha|^2$  and  $-ig\alpha(\beta^* + \beta)$ ] will result in the generation of new photons with different frequencies. When the laser-fields are incident upon the cavity, the driving energy will be transferred to a series of sidebands with new frequencies, which can be expressed as

$$x_p = \sum_{j=1}^N x_{p+}^{(j)} e^{-ij\delta_p t} + x_{p-}^{(j)} e^{ij\delta_p t}, \quad (7)$$

$$x_f = \sum_{k=1}^M x_{f+}^{(k)} e^{-ik\delta_f t} + x_{f-}^{(k)} e^{ik\delta_f t}, \quad (8)$$

similarly to the sum and difference frequency generations in the nonlinear medium, a series of sum and difference sidebands will be generated, which can be written as

$$x_s = \sum_{j=1}^N \sum_{k=1}^M x_{s+}^{(j,k)} e^{-i(j\delta_p+k\delta_f)t} + x_{s-}^{(j,k)} e^{i(j\delta_p+k\delta_f)t}, \quad (9)$$

$$x_d = \sum_{j=1}^N \sum_{k=1}^M x_{d+}^{(j,k)} e^{-i(j\delta_p-k\delta_f)t} + x_{d-}^{(j,k)} e^{i(j\delta_p-k\delta_f)t}. \quad (10)$$

By solving Eqs.(4)-(5) with the help of the ansatz (6), and using the input-output relation [32]  $S_{out} = S_{in} - \sqrt{2\kappa\alpha} (S_{in} = \varepsilon_c + \varepsilon_p e^{-i\delta_p t} + \varepsilon_f e^{-i\delta_f t})$ , we can finally obtain the output spectrum of the system

$$S_{out} = S_0 + S_p + S_f + S_s + S_d, \quad (11)$$

in which we have assumed that the detunings between the probe fields and the control field satisfy: (i)  $\delta_p = \omega_b$ ; (ii)  $\delta_f = \frac{\omega_b}{n}$  ( $n$  is a positive integer number). It should be noted that the spectrum obtained have shifted the frequency  $\omega_c$ , because Eqs.(4)-(5) describe the evolution of the optical field in a frame rotating at the control frequency. The output spectrum includes the following five parts, as shown in Fig.1(b), the first part  $S_0 = \varepsilon_c - \sqrt{2\kappa\alpha_0}$  is the 0-order sideband which corresponds to the control field  $\omega_c$ . The second and third parts denote the non-zero integer- and fraction-order sidebands, respectively, which can be expressed as

$$S_p = \sum_{j=1}^N A_{p+}^{(j)} e^{-ij\omega_b t} + A_{p-}^{(j)} e^{ij\omega_b t}, \quad (12)$$

$$S_f = \sum_{k=1}^M A_{f+}^{(k)} e^{-i\frac{k}{n}\omega_b t} + A_{f-}^{(k)} e^{i\frac{k}{n}\omega_b t}, \quad (13)$$

we will see a series of sidebands appear at  $\omega = \pm j\omega_b$  and  $\omega = \pm \frac{k}{n}\omega_b$ , in which  $A_{p+}^{(1)}$  and  $A_{f+}^{(1)}$  is called the 1- and  $\frac{1}{n}$ -order sideband, which correspond to the probe field  $\omega_p$  and  $\omega_f$ , respectively. The fourth and fifth parts describe the sum and difference sidebands, respectively, which are given by

$$S_s = \sum_{j=1}^N \sum_{k=1}^M A_{s+}^{(j,k)} e^{-i\frac{jn+k}{n}\omega_b t} + A_{s-}^{(j,k)} e^{i\frac{jn+k}{n}\omega_b t}, \quad (14)$$

$$S_d = \sum_{j=1}^N \sum_{k=1}^M A_{d+}^{(j,k)} e^{-i\frac{jn-k}{n}\omega_b t} + A_{d-}^{(j,k)} e^{i\frac{jn-k}{n}\omega_b t}. \quad (15)$$

That means a series of new sidebands will appear at  $\omega = \pm \frac{jn\pm k}{n}\omega_b$ , and we call  $A_{s\pm}^{(j,k)}$  and  $A_{d\pm}^{(j,k)}$  as the  $\pm \frac{jn\pm k}{n}$ - and  $\pm \frac{jn-k}{n}$ -order sidebands, respectively. If all the generated nonlinear sidebands appear in the output spectrum with equal interval, then they will form an optical frequency comb (OFC), and we call it as optomechanically induced sideband comb (OMISC).

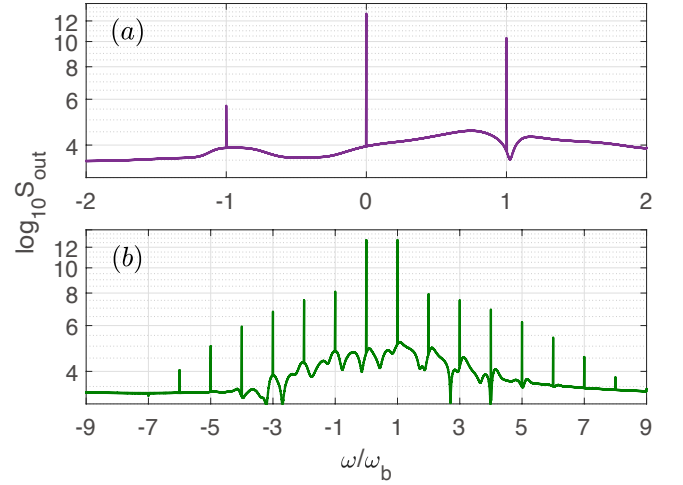


FIG. 2. (color online) The integer-order sideband spectra for different  $\varepsilon_p$ , (a)  $\varepsilon_p = 9$  GHz, (b)  $\varepsilon_p = 3 \times 10^3$  GHz, the other parameters are stated in the text.

It can be seen that it is very difficult and tedious to give the analytical solutions of the sidebands for every orders. To verify our theory and exhibit all the generated sidebands, a more convenient practice is to use the numerical calculation, and we adopt the Runge-Kutta method to solve Eqs.(4)-(5), then the output spectrum can be obtained by using the fast Fourier transform. The used parameters are chosen based on the recent experiment [33] and can be achieved under current technology:  $\omega_b/2\pi = 51.8$  MHz and  $\gamma/2\pi = 41$  kHz (quality factor  $Q_m = 1.26 \times 10^3$ ),  $m = 20$  ng,  $\Delta_a = \omega_b$ ,  $\kappa/2\pi = 15$  MHz,  $g/2\pi = 1$  kHz, the wavelength of the control field  $\lambda_c = 795$  nm, and  $\varepsilon_c = 3 \times 10^3$  GHz.

*Extending the frequency range of OMISC-* To exhibit the nonlinear sidebands output from COMS and the generation of OMISC, we firstly assume that  $\varepsilon_f = 0$  and show the integer-order (higher-order) sideband spectra in Fig. 2. We can see that when  $\varepsilon_p$  is weak ( $\varepsilon_p/\varepsilon_c = 3 \times 10^{-2}$ ), there are only 0-order and  $\pm 1$ -order sidebands in the output spectrum. If we increase  $\varepsilon_p$  and when  $\varepsilon_p$  is strong ( $\varepsilon_p/\varepsilon_c = 1$ ), the amplitudes of  $\pm 1$ -order sidebands are strengthened, and the higher integer-order sidebands appear, the positive and negative sidebands end up at the orders of +8 and -6, respectively. Furthermore, for higher order of the sideband, the amplitude is smaller. In general, both the sideband cutoff-order number and the amplitude will gradually increase with the increasing of  $\varepsilon_p$ . However, the sideband interval does not change and is always  $\omega_b$ . From the point of view of OFC, the integer-order sidebands discussed above constitute an OMISC. The frequency range  $f_r$  can be extended by increasing  $\varepsilon_p$ . For example, with the increase of  $\varepsilon_p$ ,  $f_r$  can be extended from  $[-\omega_b, +\omega_b]$  (Fig. 2(a)) to  $[-6\omega_b, +8\omega_b]$  (Fig. 2(b)), whereas the repetition frequency  $f_{rep}$  remains  $\omega_b$ .

*Decreasing the repetition frequency of OMISC-* Below

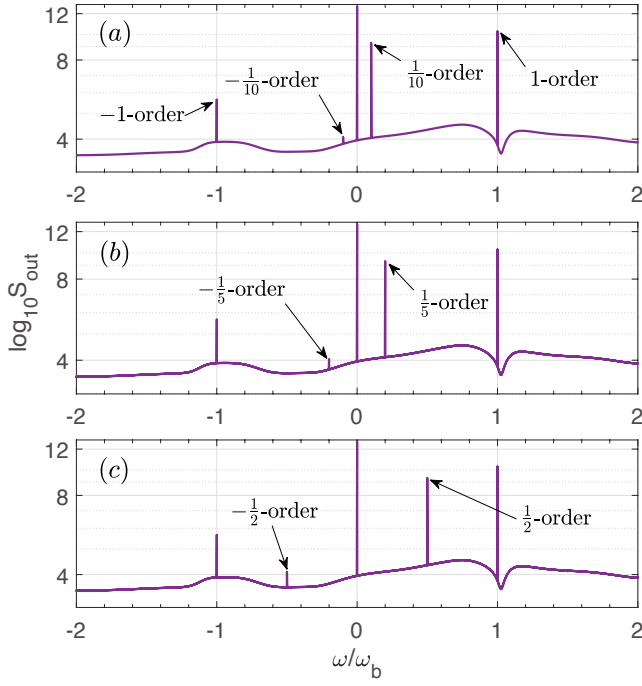


FIG. 3. (color online) The integer-order and fraction-order sideband spectra for different  $n$ , (a)  $n = 10$ , (b)  $n = 5$ , (c)  $n = 2$ .  $\varepsilon_f = 9 \times 10^{-1}$  GHz, and the other parameters are the same as that in Fig. 2(a).

we show the integer-order and fraction-order sideband spectra for different  $n$ , as shown in Fig. 3, we consider that another probe field  $\omega_f$  is inputted into the cavity with a very small amplitude ( $\varepsilon_f/\varepsilon_c = 3 \times 10^{-3}$ ), and the other conditions are the same as that in Fig. 2(a). It can be seen that the integer-order sidebands have hardly changed, while two new fraction-order sidebands appear, and their positions depend on  $n$ . Especially when  $n = 2$ , the new generated  $\pm\frac{1}{2}$ -order sidebands and the pre-existing 0-order and  $\pm 1$ -order sidebands constitute an OMISC with a smaller repetition frequency  $f_{rep} = \omega_b/2$ . However, the frequency range  $f_r$  remains  $[-\omega_b, \omega_b]$ .

Figure 4 displays the higher integer-order, fraction-order, sum and difference sideband spectra for different  $\varepsilon_f$ , and the other conditions are the same as that in Fig. 2(b). When  $\varepsilon_f/\varepsilon_c = 3 \times 10^{-2}$ , the amplitudes of  $\pm\frac{1}{10}$ -order sidebands are obviously enhanced compared with that in Fig. 3(a), and the sum and difference sidebands between  $\pm\frac{1}{10}$ -order and the integer-order sidebands, such as  $\pm\frac{11}{10}$ -order,  $\pm\frac{9}{10}$ -order,  $\pm\frac{19}{10}$ -order,  $\pm\frac{21}{10}$ -order sidebands, etc., can be seen in the output spectrum. Furthermore, the higher fraction-order sidebands, such as  $\pm\frac{2}{10}$ -order sidebands come out, and the sum and difference sidebands between  $\pm\frac{2}{10}$ -order and the integer-order sidebands can be also seen, for example,  $\pm\frac{18}{10}$ -order,  $-\frac{22}{10}$ -order sidebands, and so on. When  $\varepsilon_f/\varepsilon_c = 2 \times 10^{-1}$ , there are more higher fraction-order sidebands, such as  $\pm\frac{4}{10}$ -order sidebands, and more sum

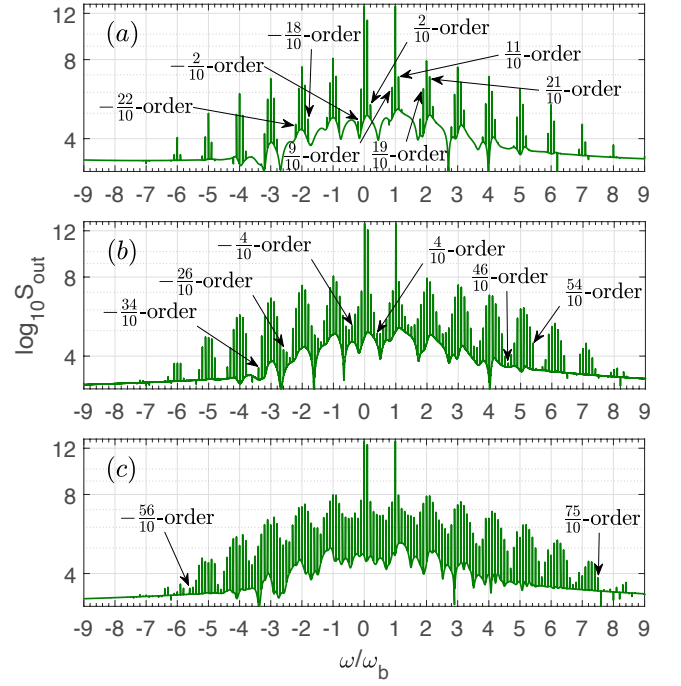


FIG. 4. (color online) The higher integer-order, fraction-order, sum, and difference sideband spectra for different  $\varepsilon_f$ , (a)  $\varepsilon_f = 9 \times 10^1$  GHz, (b)  $\varepsilon_f = 6 \times 10^2$  GHz, (c)  $\varepsilon_f = 1.2 \times 10^3$  GHz.  $n = 10$ , and the other parameters are the same as that in Fig. 2(b).

and difference sidebands, such as  $-\frac{26}{10}$ -order,  $\frac{46}{10}$ -order sidebands. All the generated nonlinear sidebands (from  $-\frac{34}{10}$ -order to  $\frac{54}{10}$ -order) constitute an OMISC with the frequency range  $f_r = [-\frac{34}{10}\omega_b, +\frac{54}{10}\omega_b]$  and repetition frequency  $f_{rep} = \omega_b/10$ . If we continue to increase  $\varepsilon_f$  and when  $\varepsilon_f/\varepsilon_c = 4 \times 10^{-1}$ , we can see that more sum and difference sidebands appear, for example,  $-\frac{56}{10}$ -order,  $\frac{75}{10}$ -order sidebands. From the angle of OMISC, in this case  $f_r$  is approximately equal to that in Fig. 2(b) while  $f_{rep}$  is decreased by one order of magnitude.

*Conclusions-* In summary, we have shown the optomechanical induced nonlinear sideband generation in a standard optomechanical system driven by three laser-fields consisting of a control field  $\omega_c$  and two probe field  $\omega_p$  and  $\omega_f$ . The detuning between  $\omega_c$  and  $\omega_p$  ( $\omega_f$ ) is equal to the mechanical frequency  $\omega_b$  ( $\omega_b/n$ ). The output sidebands can come into being an OMISC. We show that the sidebands cutoff-order number can be extended by increasing the intensity of the probe field  $\omega_p$ , which results in the enlargement of the frequency range of OMISC. In addition, the sidebands interval can be reduced by increasing  $n$  and the intensity of the probe field  $\omega_f$ , which leads to the diminution of the repetition frequency of OMISC. We conclude that the challenge to achieve the tunable OFC based on COMS will be greatly aided by our work.

This work was supported by the National Natural Science Foundation of China (Grant Nos. 61941501,

61775062, 11574092, 61475099, 61378012, and 91121023), the Program of State Key Laboratory of Quantum Optics and Quantum Optics Devices (No:KF201701), and the Doctoral Program of Guangdong Natural Science Foundation (No.2018A030310109).

---

\* wangjindong@m.scnu.edu.cn

† zhangzhiming@m.scnu.edu.cn

- [1] T. Fortier and E. Baumann, *Commun. Phys.* **2**, 1 (2019).
- [2] Y. V. Baklanov and V. P. Chebotayev, *Appl. Phys. A* **12**, 97 (1977).
- [3] J. N. Eckstein, A. I. Ferguson, and T. W. Hänsch, *Phys. Rev. Lett.* **40**, 847 (1978).
- [4] T. Rosenband, D. B. Hume, P. O. Schmidt, C. W. Chou, A. Brusch, L. Lorini, et al., *Science* **319**, 1808 (2008).
- [5] M. T. Murphy, T. Udem, R. Holzwarth, A. Sizmann, L. Pasquini, C. Araujo-Hauck, et al., *Mon. Not. R. Astron. Soc.* **380**, 839 (2007).
- [6] F. R. Giorgetta, W. C. Swann, L. C. Sinclair, E. Baumann, I. Coddington, and N. R. Newbury, *Nat. Photon.* **7**, 434 (2013).
- [7] P. Marin-Palomo, J. N. Kemal, M. Karpov, A. Kordts, J. Pfeifle, M. H. P. Pfeiffer, et al., *Nature*, **546**, 274 (2017).
- [8] S. A. Diddams, L. Hollberg, and V. Mbele, *Nature* **445**, 627 (2007).
- [9] K. Minoshima and H. Matsumoto, *Appl. Opt.* **39**, 5512 (2000).
- [10] T. M. Fortier, P. A. Roos, D. J. Jones, S. T. Cundiff, R. D. R. Bhat, and J. E. Sipe, *Phys. Rev. Lett.* **92**, 147403 (2004).
- [11] S. Schilt and T. Sdmeyer, *Appl. Sci.* **5**, 787 (2015).
- [12] W. Xia and X. Chen, *Meas. Sci. Technol.* **27**, 041001 (2016).
- [13] S. Duval, M. Bernier, V. Fortin, J. Genest, M. Pich, and R. Valle, *Optica* **2**, 623 (2015).
- [14] S. M. Link, A. Klenner, M. Mangold, C. A. Zaugg, M. Golling, B. W. Tilma, and U. Keller, *Opt. Express* **23**, 5521 (2015).
- [15] L. A. Sterczewski, J. Westberg, Y. Yang, D. Burghoff, J. Reno, Q. Hu, and G. Wysocki, *Optica* **6**, 766 (2019).
- [16] P. DelHaye, A. Schliesser, O. Arcizet, T. Wilken, R. Holzwarth, and T. J. Kippenberg, *Nature* **450**, 1214 (2007).
- [17] A. A. Savchenkov, A. B. Matsko, V. S. Ilchenko, I. Solomatine, D. Seidel, and L. Maleki, *Phys. Rev. Lett.* **101**, 093902 (2008).
- [18] V. Brasch, E. Lucas, J. D. Jost, M. Geiselmann, and T. J. Kippenberg, *Light-Sci. Appl.* **6**, e16202 (2017).
- [19] T. Herr, V. Brasch, J. D. Jost, C. Y. Wang, N. M. Kondratiev, M. L. Gorodetsky, and T. J. Kippenberg, *Nat. Photon.* **8**, 145 (2014).
- [20] A. A. Savchenkov, A. B. Matsko, V. S. Ilchenko, I. Solomatine, D. Seidel, and L. Maleki, *Phys. Rev. Lett.* **101**, 093902 (2008).
- [21] A. A. Savchenkov, A. B. Matsko, V. S. Ilchenko, D. Seidel, and L. Maleki, *Opt. Lett.* **36**, 3338 (2011).
- [22] M. A. Miri, G. DAguanno, and A. Al, *New J. Phys.* **20**, 043013 (2018).
- [23] H. Xiong, L. G. Si, X. Y. L, X. X. Yang, and Y. Wu, *Opt. Lett.* **38**, 353 (2013).
- [24] H. Xiong, L. G. Si, X. Y. L, X. X. Yang, and Y. Wu, *Ann. Phys-New York* **349**, 43 (2014).
- [25] C. Kong, H. Xiong, and Y. Wu, *Phys. Rev. A* **95**, 033820 (2017).
- [26] Z. X. Liu, H. Xiong, and Y. Wu, *Phys. Rev. A* **97**, 013801 (2018).
- [27] J. Yao, Y. F. Yu, and Z. M. Zhang, *Chin. Opt. Lett.* **16**, 111201(2018).
- [28] L. Y. He, *Phys. Rev. A* **99**, 033843 (2019).
- [29] S. Huang and G. S. Agarwal, *Phys. Rev. A* **81**, 033830 (2010).
- [30] H. Xiong, Y. W. Fan, X. X. Yang, and Y. Wu, *Appl. Phys. Lett.* **109**, 061108 (2016).
- [31] H. Xiong, Z. X. Liu, and Y. Wu, *Opt. Lett.* **42**, 18 (2017).
- [32] C. W. Gardiner and M. J. Collett, *Phys. Rev. A* **31**, 3761 (1985).
- [33] S. Weis, R. Rivière, S. Deléglise, E. Gavartin, O. Arcizet, A. Schliesser, and T. J. Kippenberg, *Science* **330**, 1520 (2010).